UNIVERSITY OF SOUTH CAROLINA

In-Plane Tow Deformations Due to Steering in Automated Fiber Placement

AIAA – SciTech 2019

Roudy Wehbe, Ramy Harik, Zafer Gürdal

Outline

I. Introduction
   A. Introduction to AFP
   B. Tow deformations due to steering
II. Problem Formulation
   A. Governing equations
   B. Numerical solution approach
III. Results
   A. Steering boundary conditions
   B. Results for a compressive region
   C. Results for a tensile region
   D. Effect of the stiffness of the foundation
   E. Effect of the steering radius
IV. Conclusions and Future Work
V. Acknowledgments and References

UNIVERSITY OF SOUTH CAROLINA

Introduction

A. Introduction to AFP
B. Tow deformations due to steering

Introduction to AFP

UNIVERSITY OF SOUTH CAROLINA

- Automated Fiber Placement (AFP) is an **additive** process used to manufacture large composites **aerospace** structures.
- During the process, up to 32 **finite width** slit-tapes or tows are deposited by the machine head within a prescribed path.
- During the process, the layup **speed**, **temperature**, roller **compaction**, and **tow tension** are controlled to obtain a good layup quality.
- Tow **steering** is required to fabricate **curved** shells and **variable stiffness** plates.
- During the steering, the **straight** tows have to **deform** to adhere to the **curved path** on the tool surface.

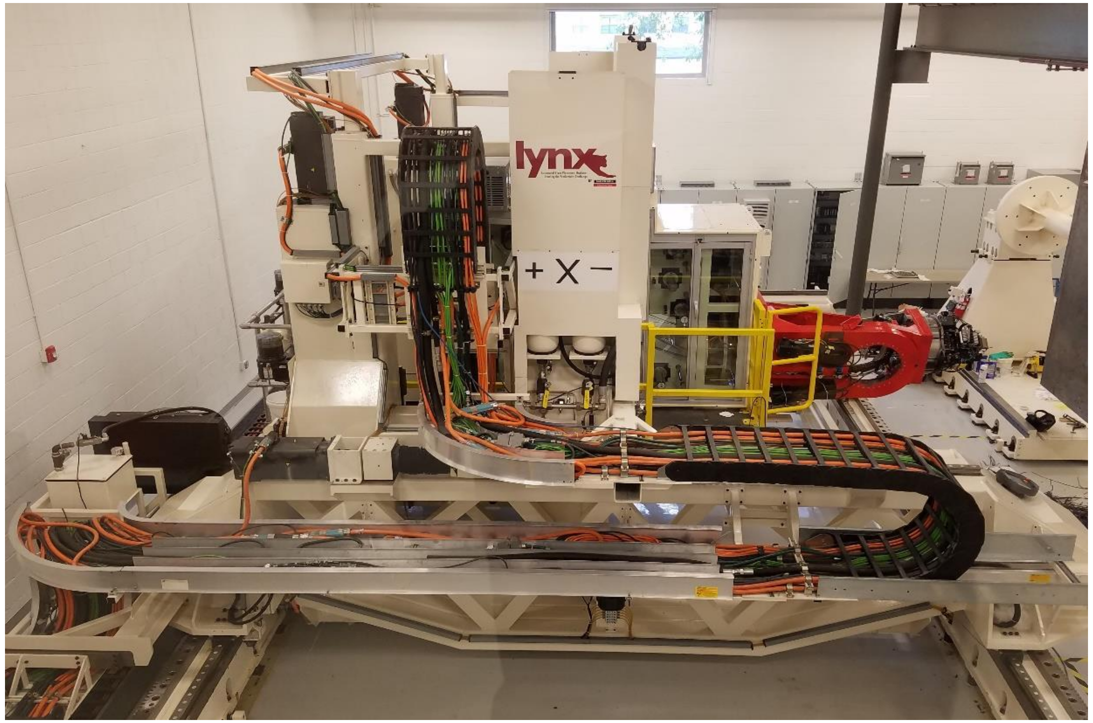

AFP machine at the McNair Center

Tow deformations due to steering

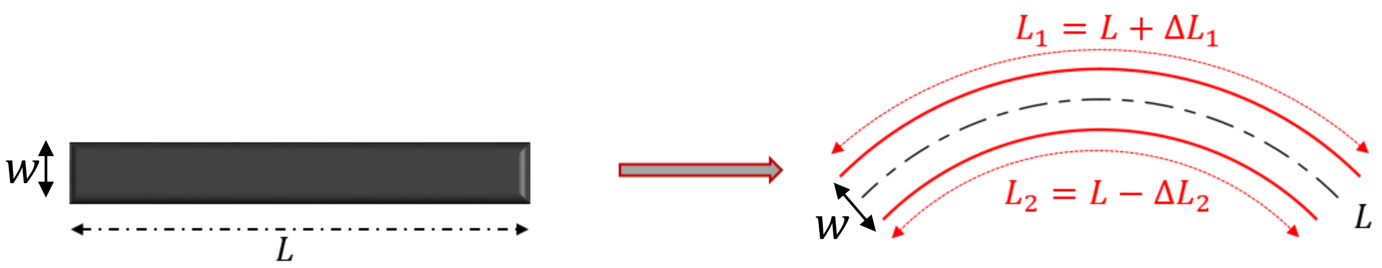

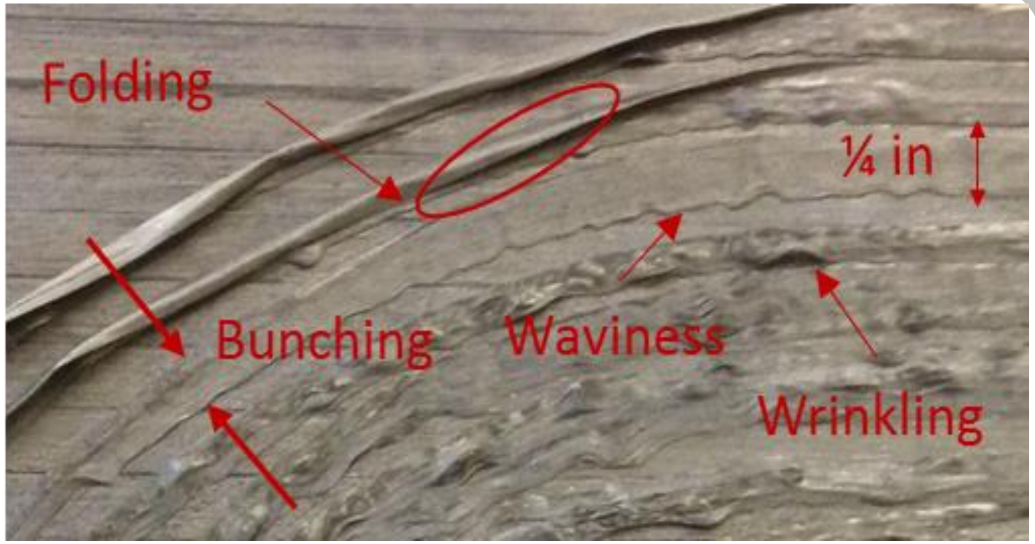

Possible deformation mechanisms

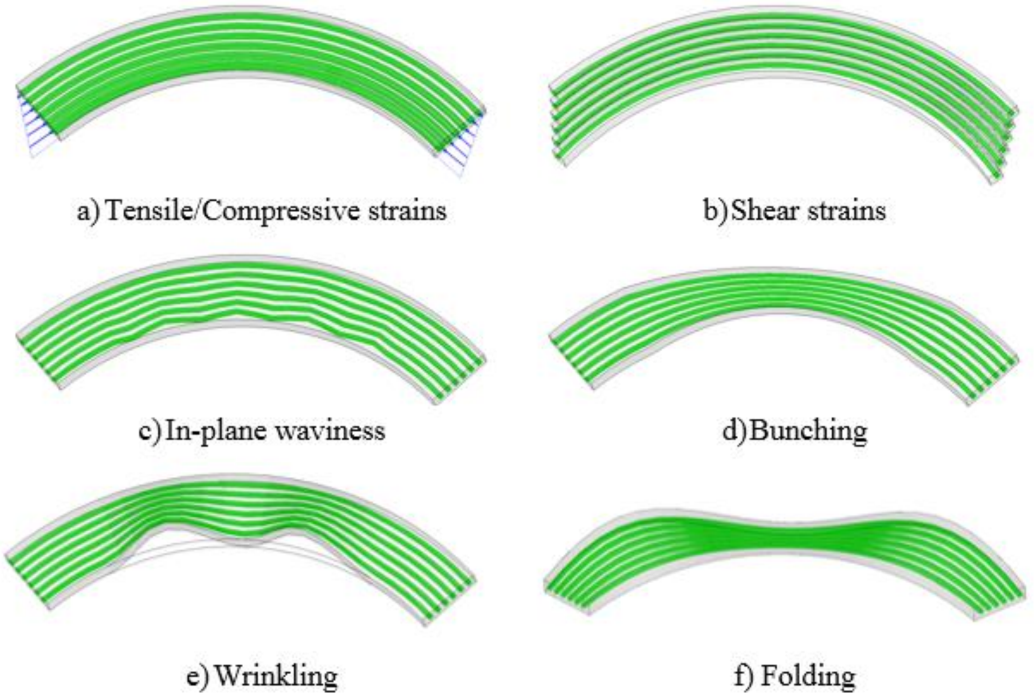

- Several deformation mechanisms are possible due to the mismatch of length between the tow and the prescribed path:
  - Elastic strain deformations
  - Large in-plane deformations
  - Large out-of-plane deformations
- The objective is to investigate the **in-plane deformations** with respect to the boundary conditions, material properties, and other process parameters.

Problem Formulation

A. Governing equation
B. Numerical solution approach

Problem formulation

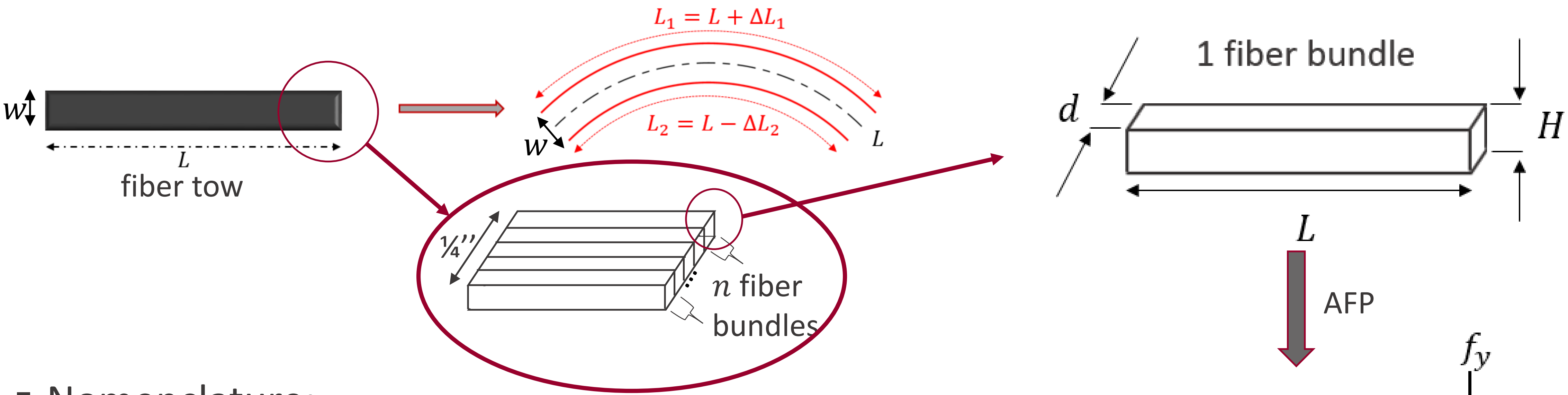

- Nomenclature:
  - γ, γ': in-plane rotation angle and in-plane curvature
  - l': axial strain
  - k_x, k_y: stiffness of the foundation (substrate) in the X an Y direction
  - f_x, f_y: forces at the endpoint
  - u, v: displacements in the X and Y direction
  - E_{11}: Elastic modulus in the fiber direction

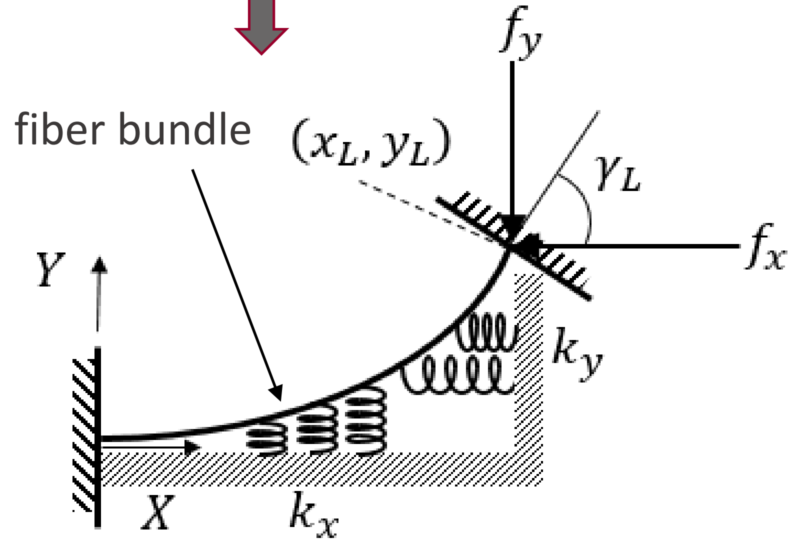

2D representation of a fiber bundle on stiff foundation

Problem Formulation

UNIVERSITY OF SOUTH CAROLINA

Minimizing the total energy of the system, subject to the BCs constraints:

$$\Pi = U - W + K$$

Elastic Strain Energy

Work

Stored Energy

BCs @ s = L:

$$\gamma(L) = \gamma_L$$

$$x(L) = x_L$$

$$y(L) = y_L$$

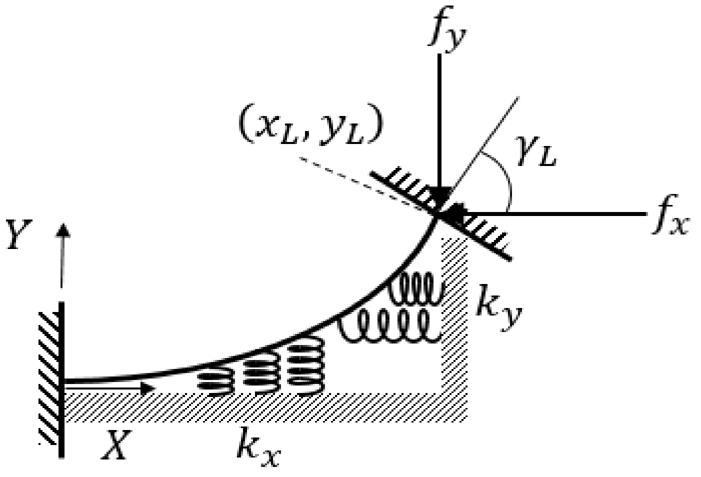

2D representation of a fiber bundle on stiff foundation

Stored Energy

$$K = \frac{1}{2}\int_0^L k_x\, u^2(s)\, ds + \frac{1}{2}\int_0^L k_y\, v^2(s)\, ds$$

Work

$$W = \boldsymbol{F} \cdot \boldsymbol{\Delta}$$

$$\boldsymbol{F} = \{f_x, f_y\} \qquad \boldsymbol{\Delta} = \{(x_L - x_0) - L, (y_L - y_0) - 0\}$$

$$x_L - x_0 = \int_0^L (1 + l')\cos\gamma \;\, ds \qquad y_L - y_0 = \int_0^L (1 + l')\sin\gamma \;\, ds$$

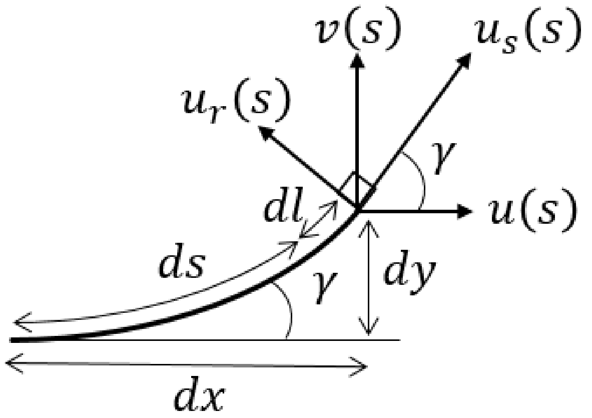

Strain-rotation relationship and displacement components

$$W = f_x\left[\int_0^L (1 + l^{'})\cos\gamma \;\, ds - L\right] + f_y\int_0^L (1 + l^{'})\sin\gamma \;\, ds$$

Governing Equations

- The strain energy of a thin composite laminate structure can be expressed as:

$$U = \frac{1}{2}\iint \left[A_{11}{\epsilon_s^o}^2 + 2A_{12}\epsilon_s^o\epsilon_r^o + A_{22}{\epsilon_r^o}^2 + A_{66}{\gamma_{sr}^o}^2 + D_{11}{\kappa_s^o}^2 + 2D_{12}\kappa_s^o\kappa_r^o + D_{22}{\kappa_r^o}^2 + D_{66}{\kappa_{sr}^o}^2\right] ds\,dr$$

- Only consider in-plane deformations, and assume the uncured tow is highly anisotropic:

$$A_{11} \gg A_{12}, A_{22}, A_{66} \quad \Rightarrow \quad U = \frac{1}{2}\int_0^L \int_{-\frac{w}{2}}^{\frac{w}{2}} A_{11}\,{\epsilon_s^o}^2\,dr\,ds$$

- Small strains, but large rotations: $\epsilon_s^o = l'(s) - r\,\kappa_r^o(s)$
- For a single layer: $A_{11} = Q_{11}H \cong E_{11}H$

Elastic Strain Energy

$$U = \frac{1}{2}\int_0^L E_{11}\left(A\,l'^2(s) + I\,\gamma'^2(s)\right) ds$$

Total Energy

$$\Pi = \frac{1}{2}\int_0^L \left(E_{11}Al'^2 + E_{11}I\gamma'^2\right) ds - f_x\left[\int_0^L (1+l')\cos\gamma\ ds - L\right] - f_y\int_0^L (1+l')\sin\gamma\ ds + \frac{k_x}{2}\int_0^L u^2(s)\,ds + \frac{k_y}{2}\int_0^L v^2(s)\,ds$$

Governing Equations

- The total energy Π contains:
  - 4 unknown functions: $\gamma(s),\ l(s), x(s), y(s)$
  - 2 unknown end forces: f_x, f_y
- $x(s)$and $y(s)$ can be expressed in terms of the strains and rotation by:

$$x' = (1 + l')\cos\gamma$$
$$y' = (1 + l')\sin\gamma$$

- Π is a functional of the form:

$$\Pi(\gamma(s), l(s)) = \int_0^L \mathcal{F}(s, \gamma(s), \gamma'(s), l'(s))\, ds$$

- Euler-Lagrange equations to minimize the energy

$$\begin{cases} \dfrac{d}{ds}\left(\dfrac{\partial \mathcal{F}}{\partial \gamma'}\right) - \dfrac{\partial \mathcal{F}}{\partial \gamma} = 0 \\ \dfrac{d}{ds}\left(\dfrac{\partial \mathcal{F}}{\partial l'}\right) - \dfrac{\partial \mathcal{F}}{\partial l} = 0 \end{cases}$$

- Governing Equations:

$$\boldsymbol{System}(f_x, f_y, s) = \begin{cases} E_{11} I\, \gamma'' - f_x(1 + l')\sin\gamma + f_y(1 + l')\cos\gamma + k_x u\, y - k_y v\, x = 0 \\ E_{11} A\, l' = F + f_x\cos\gamma + f_y\sin\gamma - k_x u\, x - k_y v\, y \\ x' = (1 + l')\cos\gamma \\ y' = (1 + l')\sin\gamma \end{cases}$$

- 5 BCs are needed to solve the system above:
  - Start point: @ $\mathrm{s} = 0$: $\gamma(0) = l(0) = x(0) = y(0) = 0$
  - End point: @ $\mathrm{s} = \mathrm{L}$: $\gamma(L) = \gamma_L$

Numerical solution approach

- Introduce error function to satisfy the remaining 2 minimization constraints x_L and y_L:

$$\boldsymbol{G}(f_x, f_y) = \begin{Bmatrix} x^*(f_x, f_y) - x_L \\ y^*(f_x, f_y) - y_L \end{Bmatrix} = \boldsymbol{0}$$

- x* and y* are the solutions of the system @ s=L
- Use Newton-Raphson method for $G(f_x, f_y)$ iteratively to find the unknown forces:

$$\begin{Bmatrix} f_{x_{n+1}} \\ f_{y_{n+1}} \end{Bmatrix} = \begin{Bmatrix} f_{x_n} \\ f_{y_n} \end{Bmatrix} - c\, J^{-1}\left(f_{x_n}, f_{y_n}\right) \boldsymbol{G}\left(f_{x_n}, f_{y_n}\right)$$

- J is the Jacobian matrix for the vector G, and can be approximated using finite difference techniques

$$J = \begin{bmatrix} \dfrac{\partial \boldsymbol{G}\left(f_{x_n}, f_{y_n}\right)}{\partial f_x} & \dfrac{\partial \boldsymbol{G}\left(f_{x_n}, f_{y_n}\right)}{\partial f_y} \end{bmatrix}$$

$$\cong \begin{bmatrix} \dfrac{\boldsymbol{G}\left(f_{x_n} + \delta, f_{y_n}\right) - \boldsymbol{G}\left(f_{x_n} - \delta, f_{y_n}\right)}{2\delta} & \dfrac{\boldsymbol{G}\left(f_{x_n}, f_{y_n} + \delta\right) - \boldsymbol{G}\left(f_{x_n}, f_{y_n} - \delta\right)}{2\delta} \end{bmatrix}$$

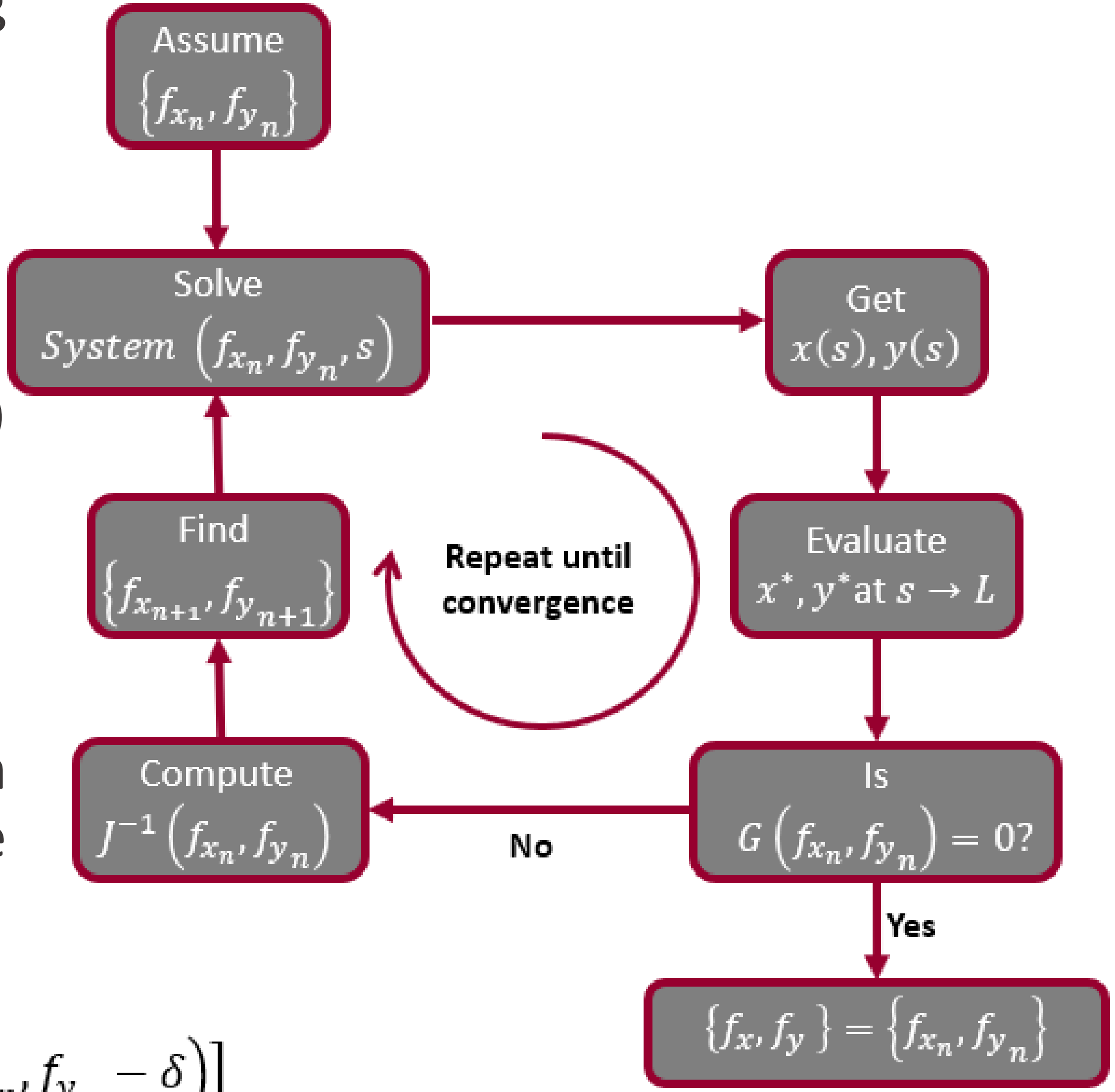

UNIVERSITY OF SOUTH CAROLINA

Results

A. Steering boundary conditions
B. Results for a compressive region
C. Results for a tensile region
D. Effect of the stiffness of the foundation
E. Effect of the steering radius

Steering Boundary Conditions

UNIVERSITY OF SOUTH CAROLINA

- For demonstration, A constant curvature tow-path is considered for analysis:

$$C(s) = \{x(s), y(s)\} = \begin{cases} \rho \ \sin\dfrac{s}{\rho} \\ \rho\left(1 - \ \cos\dfrac{s}{\rho}\right) \end{cases}, \quad 0 \le s \le L$$

- The parallel edges of the tow-path are expressed as:

$$C_p(s) = \{x_p(s), y_p(s)\} = \begin{cases} (d+\rho)\sin\dfrac{s}{\rho} \\ \rho - (d+\rho)\cos\dfrac{s}{\rho} \end{cases}$$

- The end-point BCs can be obtained from:

$$\begin{cases} x_L = x_p(L) \\ y_L = y_p(L) + d \\ \tan\gamma_L = \dfrac{y_p'(L)}{x_p'(L)} \end{cases}$$

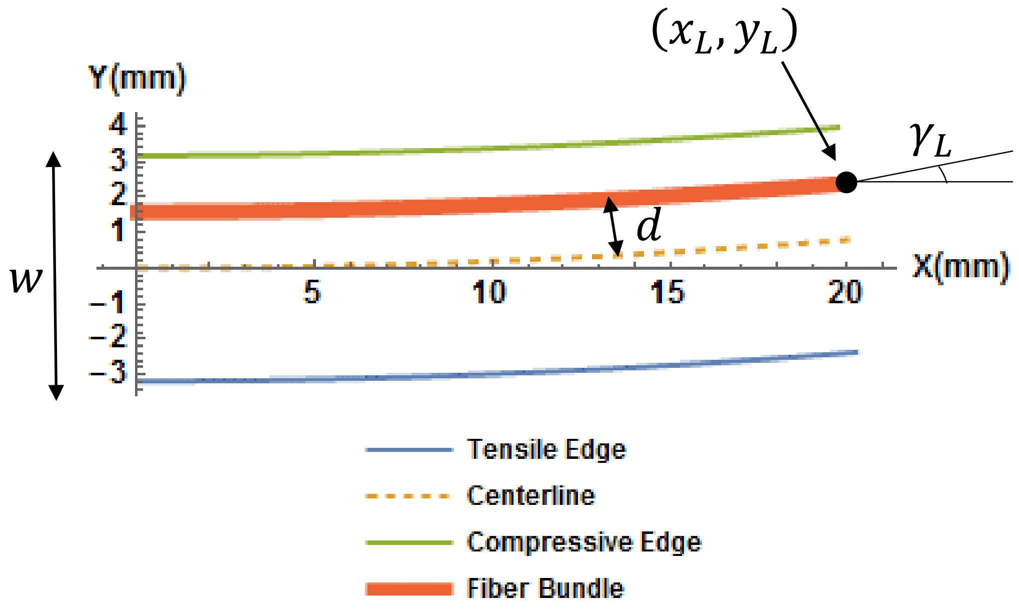

Constant curvature tow-path

Results for a compressive region

- Material Properties and tow geometry
  - $\rho = 0.4\ m$
  - $E_{11} = 130\ GPa$
  - $H = 0.184\ mm$
  - $\mathrm{w} = 6.35\ mm$
  - $k_x = k_y = 0$
- Solution of the system @ $L = 20\ mm$

Deformed fiber bundles under compression at different length

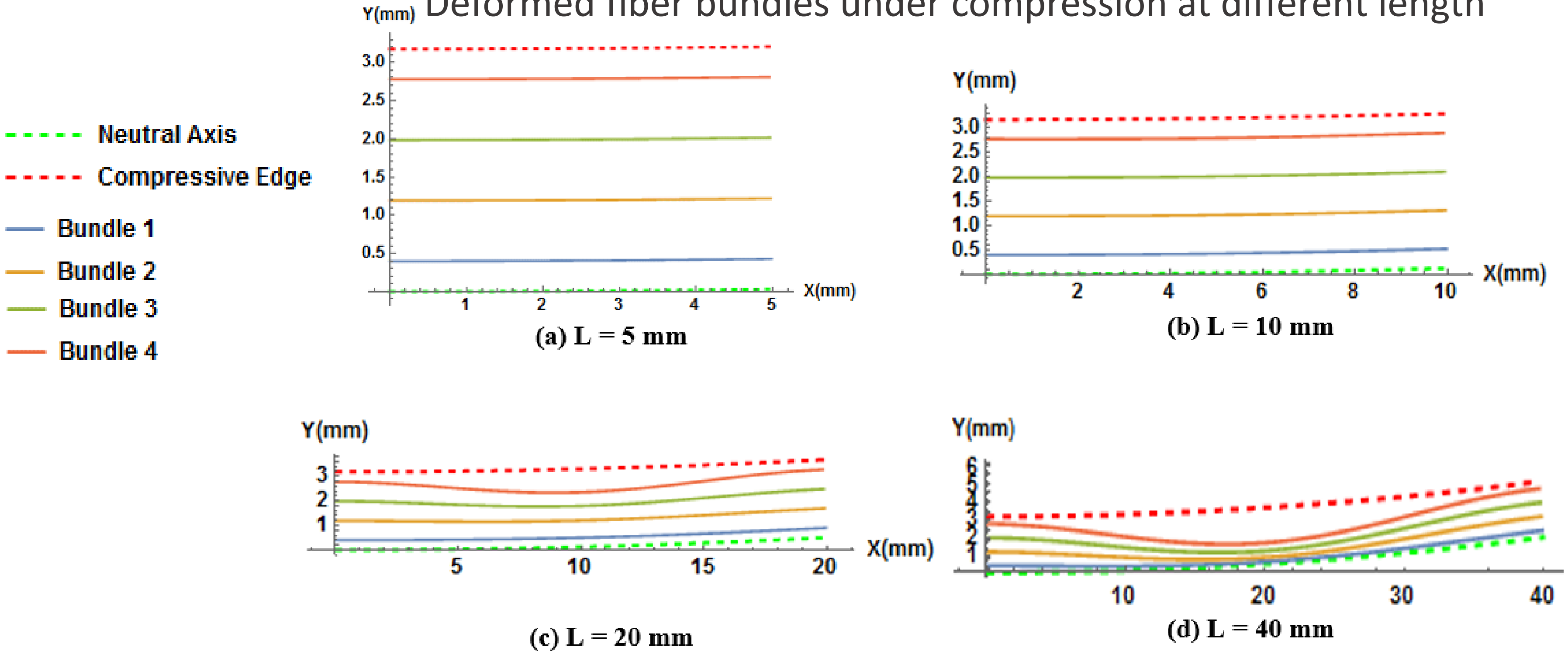

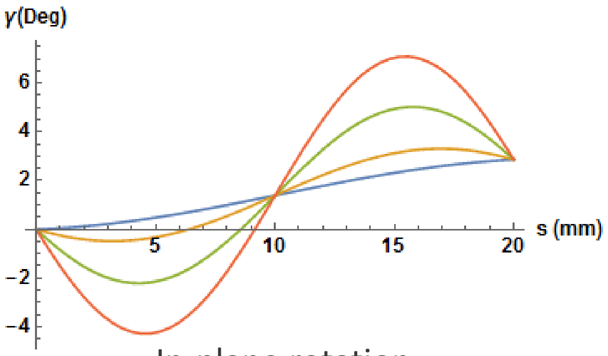

In-plane rotation

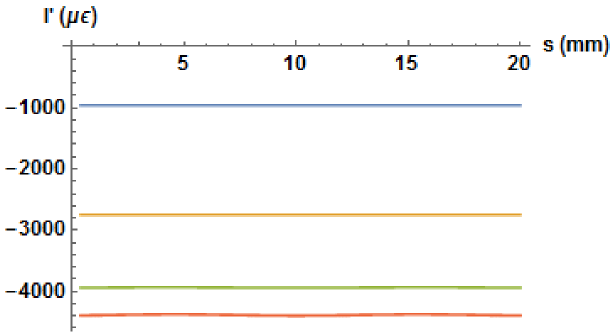

Strain along the length

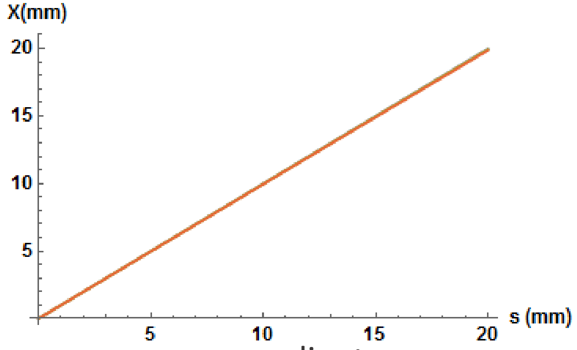

x-coordinate

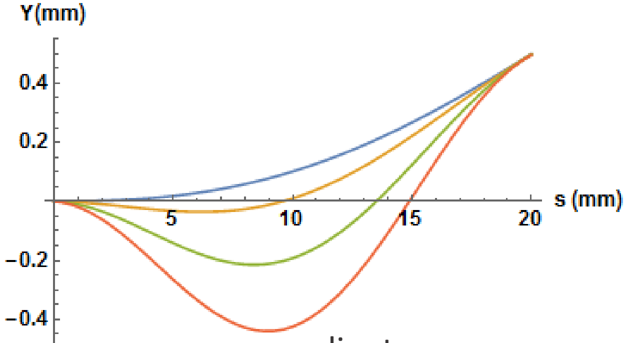

y-coordinate

Results for a tensile region

- Material Properties and tow geometry
  - $\rho = 0.4\ m$
  - $E_{11} = 130\ GPa$
  - $H = 0.184\ mm$
  - $\mathrm{w} = 6.35\ mm$
  - $k_x = k_y = 0$
- Solution of the system @ $L = 40\ mm$

Deformed fiber bundles under compression at different length

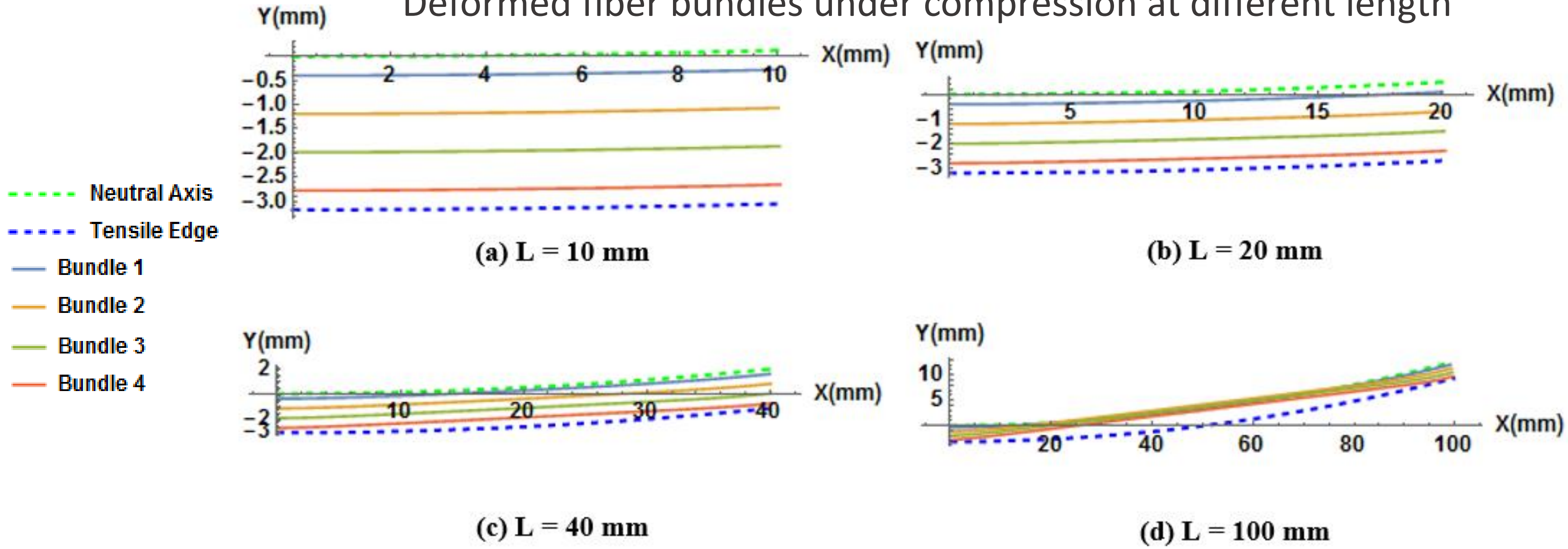

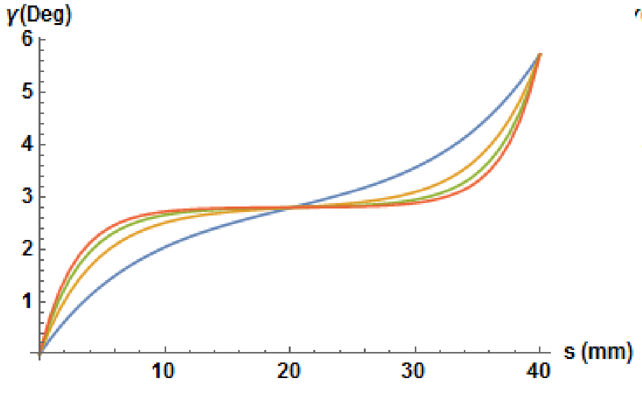

In-plane rotation

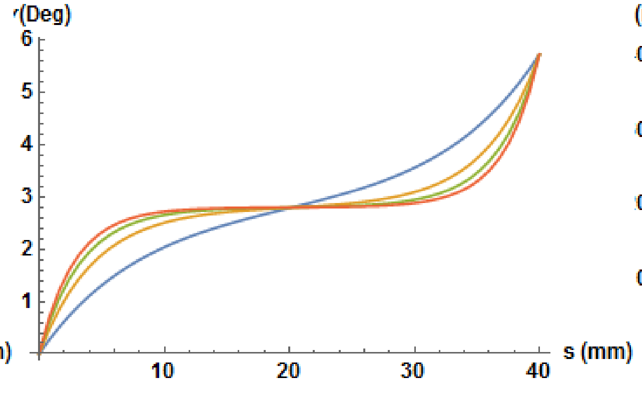

Strain along the length

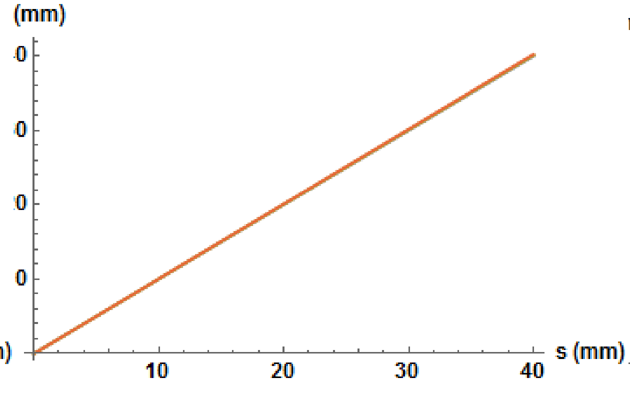

x-coordinate

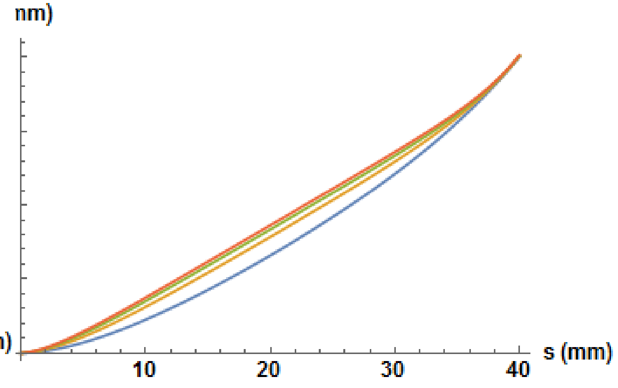

y-coordinate

Effect of the stiffness of the foundation

- Material Properties and tow geometry
  - $\rho = 0.4\ m$
  - $E_{11} = 130\ GPa$
  - $H = 0.184\ mm$
  - $\mathrm{w} = 6.35\ mm$
  - $L = 30\ mm$
  - $k_x = k_y$
- For **large values** of k ($k > 10^7\ N/m^2$):
  - $u_r \cong 0$:The fiber bundles remain in their position as placed by the AFP head
- For **small values** of k ($k < 10^6\ N/m^2$):
  - Foundation is weak and does not contribute to the fibers' deformation
- For $10^6 < k < 10^7\ N/m^2$:
  - Slight increase in u_r due to localization of the deformations

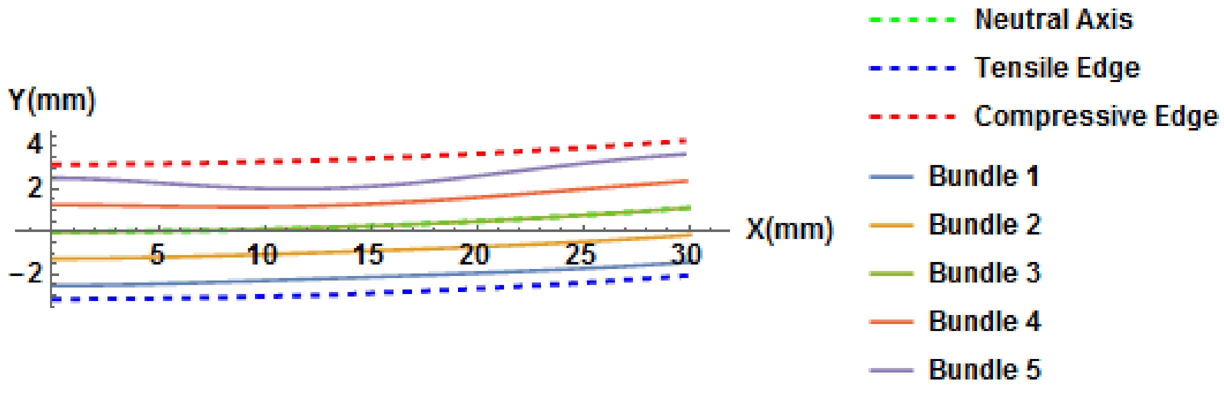

Deformed fiber bundles for $k = 10^6\ N/m^2$

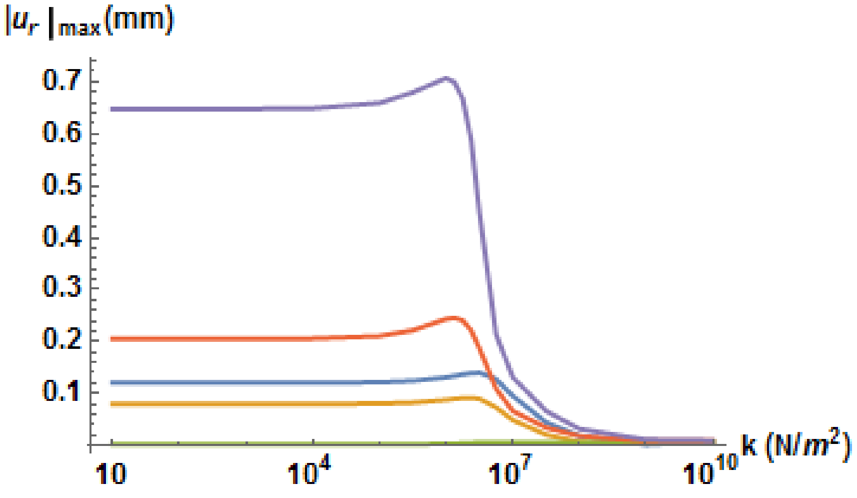

Effect of the foundation stiffness on the fibers' displacement

Effect of the steering radius

- Material Properties and tow geometry
  - $E_{11} = 130\ GPa$
  - $H = 0.184\ mm$
  - $\mathrm{w} = 6.35\ mm$
  - $L = 30\ mm$
  - $k_x = k_y$
- Increasing the steering radius decreases the displacement of the fibers in the transverse direction
- For small u_r at $k = 0$:
  - $\rho > 1.5\ m$
- For small u_r at $k = 10^7\ N/m^2$
  - $\rho > 0.5\ m$

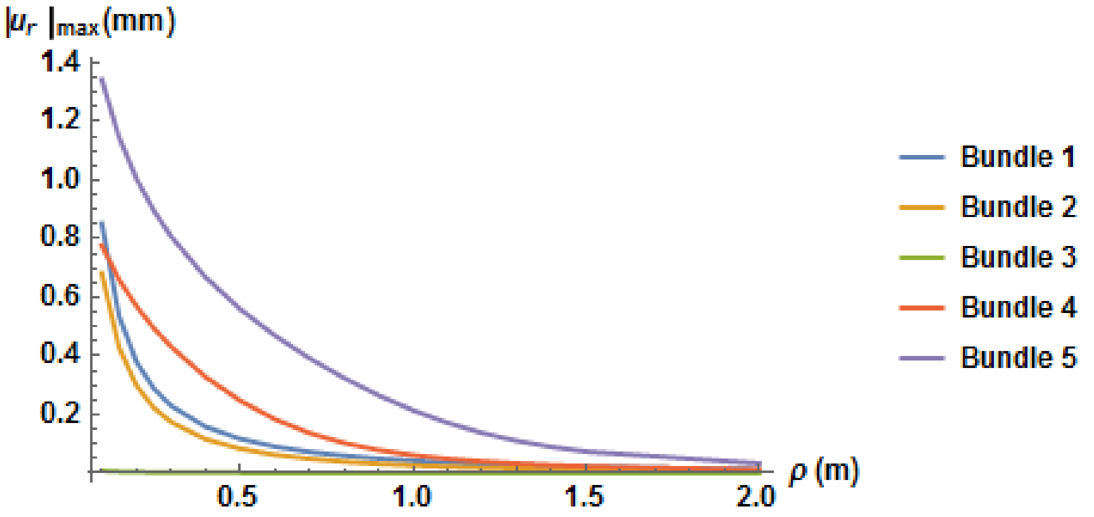

Effect of ρ on u_r for $k = 0$

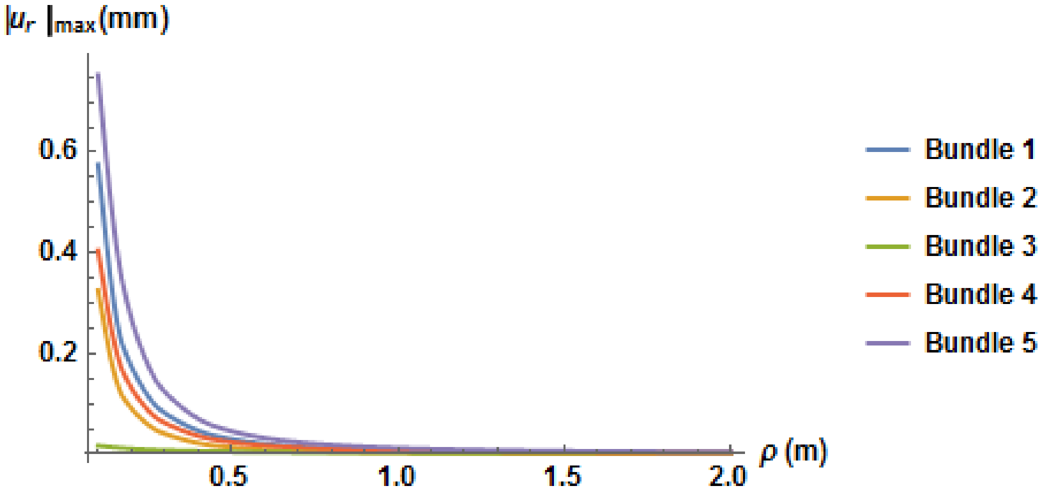

Effect of ρ on u_r for $k = 10^7\ N/m^2$

Conclusion & Future Work

Conclusion and future work

UNIVERSITY OF SOUTH CAROLINA

- The focus of this paper is to **understand** the formation of the **in-plane tow deformations** during the AFP process.
- The tow is modeled as several **fiber bundles** laying on a **stiff foundation**.
- The **governing equations** are derived based on minimizing the **total energy** of the system and a novel **numerical method** is implemented to solve the differential equations and the integral boundary constraints.
- A **constant curvature** path is considered in the analysis where the results show that at a **small length** during the additive process, **strain** deformation are **dominant** for the tensile and compressive areas within the tow.
- At **larger length**, **fiber waviness** occurs on the **compressive** side of the tow, whereas **fiber bunching/straightening** occurs on the **tensile** side of the tow.
- **Increasing** the **stiffness** of the foundation can **reduce** the in-plane deformation of the tow and possibly eliminating it for a very stiff foundation. However, steering tow at **smaller** radii of curvature **increases** the magnitude of the in-plane deformation mechanisms.
- Future work will consist of investigating the **out-of-plane deformation** mechanisms, and examining the importance of other parameters such as **shear** and **transverse** strain. **Experimental** work is necessary to determine the values of the **stiffness** of the foundation and to relate it to other process parameters such as **speed** and layup **temperature**.

Acknowledgments and References

UNIVERSITY OF SOUTH CAROLINA

- **Acknowledgments**
  - The authors would like to thank The Boeing Company for their support of this work. Also, the authors would like to thank Dr. Brian Tatting for the invaluable comments and suggestions.

- **References**

[1] Lukaszewicz, D. H. J. A., Ward, C., and Potter, K. D., "The engineering aspects of automated prepreg layup: History, present and future," *Composites Part B: Engineering*, vol. 43, 2012, pp. 997–1009.

[2] Beakou, A., Cano, M., Le Cam, J. B., and Verney, V., "Modelling slit tape buckling during automated prepreg manufacturing: A local approach," *Composite Structures*, vol. 93, 2011, pp. 2628–2635.

[3] Matveev, M. Y., Schubel, P. J., Long, A. C., and Jones, I. A., "Understanding the buckling behaviour of steered tows in Automated Dry Fibre Placement (ADFP)," *Composites Part A: Applied Science and Manufacturing*, vol. 90, 2016, pp. 451–456.

[4] Wehbe, R., "Modeling of Tow Wrinkling in Automated Fiber Placement based on Geometrical Considerations," University of South Carolina, 2017.

[5] Wehbe, R., Tatting, B. F., Harik, R., Gurdal, Z., and Miller, E., "Geometrical Modeling of Tow Wrinkles in Automated Fiber Placement," *Submitted to CAD Computer Aided Design*.

[6] Lichtinger, R., Hörmann, P., Stelzl, D., and Hinterhölzl, R., "The effects of heat input on adjacent paths during Automated Fibre Placement," *Composites Part A: Applied Science and Manufacturing*, vol. 68, 2015, pp. 387–397.

[7] Kassapoglou, C., *Design and Analysis of Composite Structures*, WILEY, 2013.

[8] Timoshenko, S. P., and Gere, J. M., *Theory of Elastic Stability*, Dover Publications, 1961.

[9] Rousseau, G., Wehbe, R., Halbritter, J., and Harik, R., "Automated Fiber Placement Path Planning: A State-of-the-art review," *Computer-Aided Design and Application*, vol. 16, 2019, pp. 172–203.